

1994

Removal of Magnetic Impurities from Strontium Copper Oxychloride

Colleen B. Eads
Iowa State University


Carol J. Kosmicke
Iowa State University

Lance L. Miller
Iowa State University

Let us know how access to this document benefits you

Copyright © Copyright 1994 by the Iowa Academy of Science, Inc.

Follow this and additional works at: <https://scholarworks.uni.edu/jias>

 Part of the [Anthropology Commons](#), [Life Sciences Commons](#), [Physical Sciences and Mathematics Commons](#), and the [Science and Mathematics Education Commons](#)

Recommended Citation

Eads, Colleen B.; Kosmicke, Carol J.; and Miller, Lance L. (1994) "Removal of Magnetic Impurities from Strontium Copper Oxychloride," *Journal of the Iowa Academy of Science: JIAS*, 101(2), 45-48.

Available at: <https://scholarworks.uni.edu/jias/vol101/iss2/5>

This Research is brought to you for free and open access by the Iowa Academy of Science at UNI ScholarWorks. It has been accepted for inclusion in Journal of the Iowa Academy of Science: JIAS by an authorized editor of UNI ScholarWorks. For more information, please contact scholarworks@uni.edu.

Removal of Magnetic Impurities from Strontium Copper Oxychloride

COLLEEN B. EADS,¹ CAROL J. KOSMICKE,²
and LANCE L. MILLER

Ames Laboratory, Iowa State University, Ames, Iowa 50011

Analyses of a copper-deficient series of Strontium Copper Oxychloride polycrystalline samples are reported. Magnetic susceptibility, X-ray powder diffraction, and differential thermal analyses show a small Curie-type magnetic signal correlates with $\approx 0.6\%$ (excess) copper ions in the nominally stoichiometric material. The analyses also imply that the extra magnetic signal is from an impurity phase, possibly related to Strontium Copper Oxide. The concentration of the impurity phase can be controlled by varying the copper stoichiometry. INDEX DESCRIPTORS: Magnetic impurity, magnetic susceptibility, $\text{Sr}_2\text{CuO}_2\text{Cl}_2$

Interest in the properties¹⁻⁸ of Strontium Copper Oxychloride ($\text{Sr}_2\text{CuO}_2\text{Cl}_2$) lies in its structural and electronic similarities to the Lanthanum Copper Oxide (La_2CuO_4)—type high temperature superconductor.⁹ Both $\text{Sr}_2\text{CuO}_2\text{Cl}_2$ and stoichiometric La_2CuO_4 have 2D antiferromagnetic short range order (AFM-SRO) in the Cu-O planes with a crossover to 3D antiferromagnetic long range order (AFM-LRO) around room temperature.² Doping Sr into La_2CuO_4 produces a 40K superconductor⁹ whereas the title compound has yet to be successfully doped.¹ It is thought that a better understanding of the mechanism of superconductivity will come from study of $\text{Sr}_2\text{CuO}_2\text{Cl}_2$.

Both compounds share the K_2NiF_4 structure type.^{1,10} $\text{Sr}_2\text{CuO}_2\text{Cl}_2$ differs from La_2CuO_4 in that the apical oxygens of the CuO_6 octahedra are replaced with Cl and the La ions replaced with Sr to balance the overall charge. There is also a tetragonal to orthorhombic phase transition⁹ in La_2CuO_4 which has not been found¹ in $\text{Sr}_2\text{CuO}_2\text{Cl}_2$.

$\text{Sr}_2\text{CuO}_2\text{Cl}_2$ has a complex magnetic behavior. 2D AFM-SRO is expected² near 900K. As the temperature lowers, the correlated regions become larger and the fluctuations slow until there is a transition² to 3D AFM-LRO at 250K. Recently a form of *static* 2D AFM-SRO has been discovered⁶ between 250 and 400K. Also, there is a cusp in the magnetization data² and a splitting of muon spin rotation frequencies,^{3,7} possibly indicating a magnetic phase transition at 40K.

In order to examine and explain the magnetic behavior, it is necessary to remove magnetic impurity contributions to the experimental data. Contributions from non-magnetic impurities barely affect the data and can be ignored. Two methods of removing the magnetic impurity signal are: A) fit the impurity signal with a calculated curve and subtract its contribution out, or B) produce samples without the magnetic impurities.

Fitting and subtracting off the impurity contribution suffers from two disadvantages. First, one must know the character of the impurity and intrinsic signals. Since this compound is still under investigation, the intrinsic signal is not entirely obvious. Second, one must be able to mathematically distinguish the impurity and intrinsic signals. This, too, is a disadvantage since the important fitting region at low temperatures has relatively rapidly varying intrinsic magnetic events which are not small compared to the impurity signal.

In this material Cu^{2+} ions are assumed to be the source of the Curie-type magnetic signal seen in the magnetization data. It is further assumed that the Cu^{2+} ions exist in a phase different from $\text{Sr}_2\text{CuO}_2\text{Cl}_2$ (as opposed to being due to lattice defects).

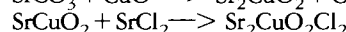
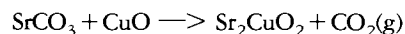
This paper reports our efforts to produce magnetically pure $\text{Sr}_2\text{CuO}_2\text{Cl}_2$. Four samples were prepared with varying degrees of

copper deficiencies. It was hypothesized that the copper deficiency would come from the impurity phase, thus reducing the magnitude of the magnetic impurity's signal. Because one loses control over the material when growing single crystals and a greater potential for lattice defects exists, all reactions and final products are in polycrystalline form. X-ray powder diffraction, Differential Thermal Analysis, and D.C. Magnetization analysis techniques were used to compare the effects that the copper deficiencies have on the properties of the final products.

EXPERIMENTAL

Sample Preparation

Preparation of $\text{Sr}_2\text{CuO}_2\text{Cl}_2$ is best accomplished¹ using the two step reaction



due to the low melting point of SrCl_2 . To minimize sample to sample stoichiometry variations, a single large batch of $\text{SrCu}_{0.994}\text{O}_2$ was first prepared. This product was then split into four batches to which CuO and SrCl_2 were added to make up the desired stoichiometries of $\text{Sr}_2\text{Cu}_{1.000}\text{O}_2\text{Cl}_2$, $\text{Sr}_2\text{Cu}_{0.998}\text{O}_2\text{Cl}_2$, $\text{Sr}_2\text{Cu}_{0.996}\text{O}_2\text{Cl}_2$, and $\text{Sr}_2\text{Cu}_{0.994}\text{O}_2\text{Cl}_2$. Hereafter, the series is referred to as $\text{Sr}_2\text{Cu}_x\text{O}_2\text{Cl}_2$ with $x = 1.000$, $x = 0.998$, $x = 0.996$, and $x = 0.994$. Note: The oxygen stoichiometry is fixed by the amount necessary for charge neutrality. O_2 is written for convenience.

$\text{SrCu}_{0.994}\text{O}_2$ was prepared by adding CuO (99.99%) to SrCO_3 (99.99%), grinding the mixture in an agate mortar and pestle, and pressing the mixture into pellet form. Firing took place in air at 925°C in a covered alumina crucible (COORS). Grinding and firing was repeated until the X-ray powder diffraction pattern remained unchanged from the previous day's pattern.

The second stage involved splitting up the $\text{SrCu}_{0.994}\text{O}_2$ into four batches to which CuO and SrCl_2 were added to produce the series. The actual formula for SrCl_2 is $\text{SrCl}_2 \cdot x\text{H}_2\text{O}$. The number of waters of hydration is dependent on storage conditions. Determination of the number of waters was carried out on a Perkin Elmer Model 7 Thermal Gravimetric Analyzer (TGA). A small amount was placed on the weighing pan and heated to 300°C in helium. Assuming the weight lost was due to water loss and that the final compound was pure SrCl_2 , the number of moles water per mole SrCl_2 was computed and used to obtain the actual molecular formula. Mixtures of the series were then ground, pressed into pellets, and heated at 800°C. X-ray powder diffraction analysis was again used to follow the reactions to completion.

DTA Analysis

Fig. 1 shows data collected on the series of samples using a Perkin

¹Current address: Martensdale-St. Marys High School Martensdale, Iowa 50160

²Current address: Valley High School, West Des Moines, Iowa 50265

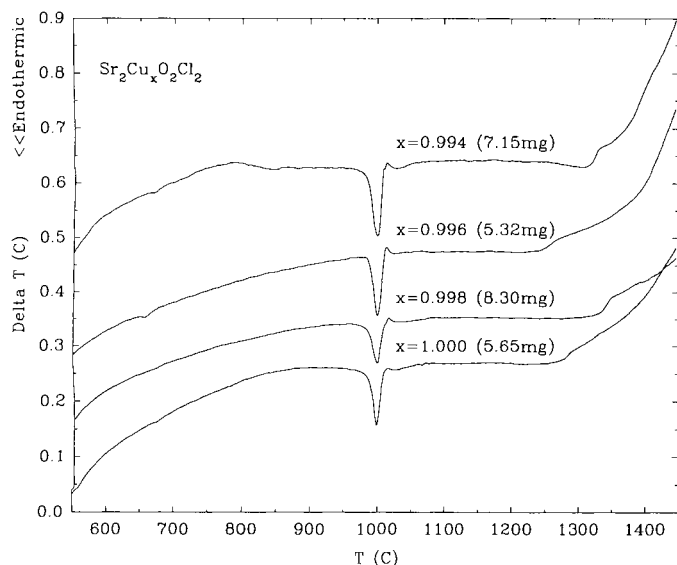


Fig. 1. Differential Thermal Analysis scans of the series $\text{Sr}_2\text{Cu}_x\text{O}_2\text{Cl}_2$ with $x = 1.000, 0.998, 0.996,$ and 0.994 .

Elmer Model 1700 Differential Thermal Analyzer (DTA). Alumina crucibles were used to contain the powdered samples since previous experience has shown no reaction between Al_2O_3 and $\text{Sr}_2\text{CuO}_2\text{Cl}_2$. Alumina powder was used above and below the samples to enhance thermal contact between the samples and the crucible and to minimize infrared heating differences between the sample-containing crucible and an identical reference crucible (without sample). The sample and reference crucibles were heated from 500 to 1400°C at 20°C/min. To simulate pure air, an atmosphere of 20% O_2 /80% He flowing at 40 cm^3/min was used. The plots show the scaled temperature difference between the sample-containing crucible and the reference crucible versus the oven temperature.

The events at 675 and 825°C show the sensitivity of the DTA to small impurities. These two events are also seen when using an empty sample holder and thus are from contamination of the crucible. The contaminant comes from handling the crucible with stainless steel tweezers and is removed by washing the crucibles with acid. The DTA profiles are also sensitive to the amount of sample used. The runs have been repeated using sample weights ranging from 5 to 35 mg. Excess amounts of sample produces broader transitions and can split the endothermic transition at 1000°C into multiple peaks. The data in Fig. 1 are from 5.32 to 8.30mg samples.

X-ray Analysis

Fig. 2 shows X-ray powder diffraction profiles for the series of four samples. Each phase has a unique set of peak positions and intensities in the profiles. The peaks belonging to $\text{Sr}_2\text{CuO}_2\text{Cl}_2$ ($a = 3.9716\text{Å}$, $C = 15.612\text{Å}$, $I4/mmm$ symmetry¹) have been labeled with their Miller indices.

The most apparent continuous change is the disappearance of the small peaks in the 2θ ranges 15-20, 24-26, 29-30, 38-39, 42-45, and 48-50°. The diminishing intensities imply that the impurity phase(s) concentration correlates with the Cu concentration. Non-systematic effects are generally due to counting statistics and preferred orientation variations typical of samples with grains having plate-like morphology.

Typically, a few percent impurity level detection limit is attained with an X-ray diffractometer. Comparison of the aforementioned impurity peaks with reference patterns was difficult due to the small signal and the breadth of the peaks. While no exact match has been

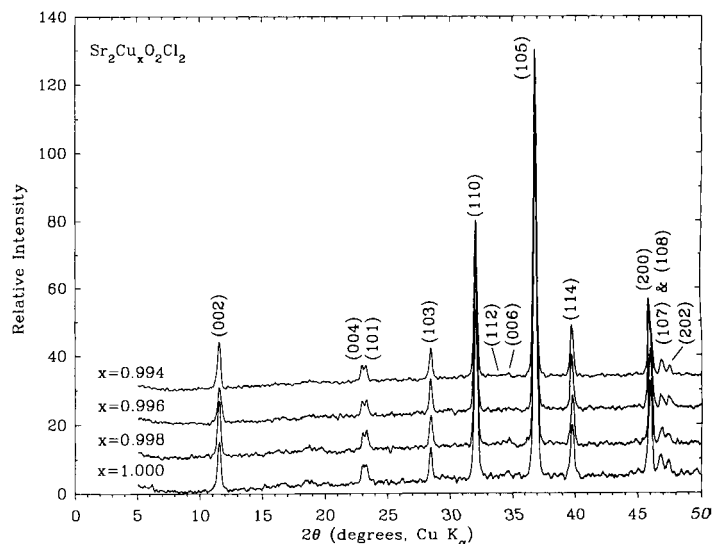


Fig. 2. X-ray powder diffraction profiles of the series $\text{Sr}_2\text{Cu}_x\text{O}_2\text{Cl}_2$ with $x = 1.000, 0.998, 0.996,$ and 0.994 . $\text{Cu K}\alpha$ radiation.

found, the impurity peaks have a pattern similar to that of SrCuO_2 and are assumed to be a closely related phase.

Magnetization Analysis

Fig. 3 shows the molar magnetic susceptibility data ($\chi_m = M/H$) for the series of powder samples. Data were collected between 5 and 150K using a Quantum Design D.C. Squid Magnetometer with an applied field of 1 Tesla. Additive constants were used for each curve to separate them while retaining the relative ordering. Symbols represent raw data, lines through the symbols are the calculated fits, and the lines near zero are the difference between the two.

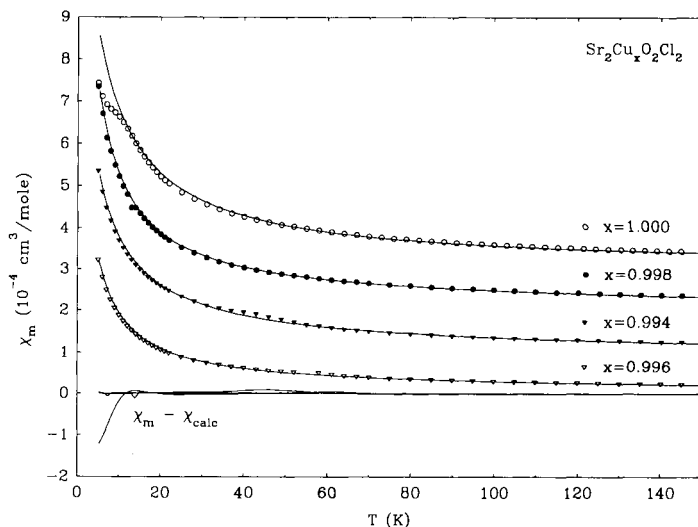


Fig. 3. Molar magnetic susceptibility ($\chi_m = M/H$) data for the series $\text{Sr}_2\text{Cu}_x\text{O}_2\text{Cl}_2$ with $x = 1.000, 0.998, 0.996,$ and 0.994 . Polycrystalline samples in an applied field of 1 Tesla. Symbols represent experimental data (χ_m), lines through symbols are calculated curves (χ_{calc}) and lines near zero are the difference ($\chi_m - \chi_{\text{calc}}$).

Previous work² showed that the data could best be described by a modified Curie-Weiss equation, viz

$$\chi_m = \chi_o + \frac{C}{T - \theta} + aT. \quad (1)$$

χ_o accounts for core electron diamagnetism, average Van Vleck paramagnetism, and a diamagnetic signal from the sample holder. C is the Curie constant due to isolated spins and the Weiss molecular field constant θ accounts for interactions between these spins. The term linear in T is necessary for a good fit and is presently presumed to account for antiferromagnetic spin waves.²

θ for these samples is small so that to a good approximation

$$\chi_m T = C + \chi_o T + aT^2. \quad (2)$$

Fig. 4 plots $\chi_m T$ versus T to highlight additional information contained in the susceptibility data. Here we see a small cusp at 57K for $x = 0.996$, $x = 0.994$, and $x = 0.998$. This cusp is due to oxygen from air trapped in the powdered samples while being readied for measurement. At 45K a broad cusp is seen in the $x = 0.994$ data and a shoulder in the $x = 1.000$ data at 10K. Less prominent features are located at 25K in all samples.

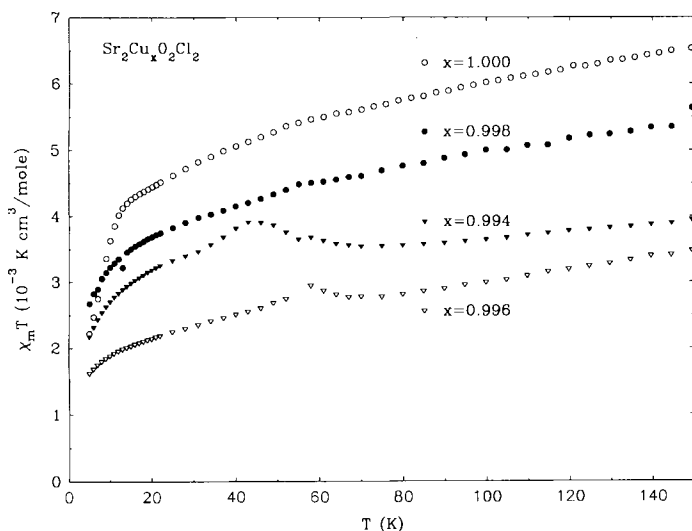


Fig. 4. $\chi_m T$ versus T graph highlighting small peaks at lower temperatures.

By excluding the larger cusps, Eqn. (1) was used in a least squares fit to the experimental data. Assuming the resulting Curie constant is due only to the magnetic impurity, the molar percent impurity concentration (%I) is computed as

$$\%I = \frac{C}{0.374} \times 100. \quad (3)$$

Further assumptions necessary in deriving Eqn. (3) are spin = 1/2, $g = 2$ (both good assumptions for a Cu^{2+} impurity), and that %I is small. The results of the fits and the computations in Eqn. (3) are given in Table 1.

DISCUSSION OF RESULTS

It has been previously determined from DTA measurements¹ that $\text{Sr}_2\text{CuO}_2\text{Cl}_2$ melts incongruently into a liquid (SrCl_2 , m.p. = 875°C) and a second solid phase (SrCuO_2 , m.p. = 1035°C) at 1000°C. Further heating melts the second solid phase and, by 1500°C, the resulting liquid has evaporated. Major events in Fig. 1 consist of an endothermic transition at 1000°C, a broad transition near 1035°C, and another ranging from 1225 to 1325°C. From this we conclude that the 1000°C

Table 1. Results from fits to experimental magnetic susceptibility data for $\text{Sr}_2\text{Cu}_x\text{O}_2\text{Cl}_2$. CGS units.

X	Excluded	χ_o	$C \times 10^3$	θ	$a \times 10^8$	%I
1.000	5 to 10K	6.18×10^{-6}	5.35	-4.58	2.38	1.43
0.998	none	1.94×10^{-9}	3.65	-2.10	-5.10	0.976
0.996	30 to 70K	1.28×10^{-5}	2.05	-1.61	-2.50	0.547
0.994	20 to 80K	6.12×10^{-6}	3.52	-3.27	-2.70	0.942

peak is the incongruent melting point of $\text{Sr}_2\text{CuO}_2\text{Cl}_2$, 1035°C is the melting point of SrCuO_2 , and the highest temperature endothermic transition is the evaporation temperature or boiling point of the final liquid.

The final evaporation temperature correlates with the sample mass. This is understandable if the liquid has a high vapor pressure and if the smaller samples evaporate completely before the boiling point is reached. This argument can also explain the character difference between runs with small amounts of sample (which evaporate before the boiling point) and runs with larger amounts of sample (which evaporate at the boiling point). Other runs (not shown) with larger sample weights confirm 1325°C is the actual boiling point.

A closer examination of Fig. 1 shows a small, sharp peak on the high-temperature side of the 1000°C transition. The appearance of this peak occurs when the sample mass increases and is thought to be an intermediate phase between SrCuO_2 and $\text{Sr}_2\text{CuO}_2\text{Cl}_2$.

A comparison of the DTA runs shows no systematic effects that correlate with an impurity phase. Clear evidence of the impurity phase was expected due to the high sensitivity of the DTA to impurities. It is possible that overlapping peaks obscure the small impurity peaks. If the impurity is SrCuO_2 , for example, the melting transition of the small impurity phase would be overwhelmed by the melting of SrCuO_2 from the incongruently melted $\text{Sr}_2\text{CuO}_2\text{Cl}_2$. It is also possible that the impurity peak(s) are broadened (and the corresponding peak height(s) lessened) or that the heat of transition is simply too small.

An impurity phase similar to SrCuO_2 is seen by X-ray diffraction. Since $\text{Sr}_2\text{CuO}_2\text{Cl}_2$ incongruently melts into SrCl_2 and SrCuO_2 , this is consistent with our inability to resolve an impurity peak via the DTA. If an excess of SrCuO_2 is present, then this could be from too little SrCl_2 being available for the reaction to be completed. This could be due to impurities in the SrCl_2 , evaporation while reacting, or SrCl_2 forming an amorphous coating on the polycrystalline grains. Further tests with lower reaction temperatures using purer, anhydrous SrCl_2 are planned.

From Table 1 we find a good correlation of decreasing impurity level with copper deficiency exists for $x = 1.000$, 0.998, and 0.996. The $x = 0.994$ results do not, however, follow the trend. Reexamination and numerous attempts to fit the $x = 0.994$ data are foiled by the broad cusps below 80K seen in Fig. 4.

For the three good fits, one observes that a 0.2% decrease in copper content lowers the calculated magnetic impurity level by about 0.5%. For $x \leq 0.9935$ a magnetic-impurity free sample is expected.

The relatively large effect that a small Cu^{2+} deficiency has on the impurity signal is striking. From this one might surmise that A) a more complicated phase mechanism than originally put forth exists, B) that an assumption inherent in Eqn. 3 is incorrect, or C) that a systematic error is induced by the magnetism of $\text{Sr}_2\text{CuO}_2\text{Cl}_2$ during the fits. Further studies at higher and lower copper concentrations could clarify this point.

The magnetic data in Figs. 3 and 4 bring to light some intriguing questions about the intrinsic nature of the cusps below 60K. The 45K cusp has been seen² in single crystals by magnetization and muon spin rotation measurements^{3,7} and has thus been thought intrinsic to this material. Here we see that the position and intensity are variable and

that more than one transition exists. Once the impurity contribution is brought to zero, investigations of these transitions will be carried out.

CONCLUSION

The results of the analyses support the initial hypothesis that the extra Curie-type magnetic signal originates in an impurity phase. A phase related to SrCuO_2 is thought to be the impurity. Fits to the magnetization data interpolate to a magnetic impurity free concentration at $x \leq 0.9935$. Extension of this work using purer, anhydrous SrCl_2 , reacting at lower temperatures, and increasing the copper deficiencies will clarify a few points and bring the magnetic impurity signal near zero.

ACKNOWLEDGEMENTS

This work was supported in part by the Program for Women in Science and Engineering, Iowa State University and in part by Ames Laboratory which is operated for the U.S. Department of Energy by Iowa State University under contract No. W-7405-ENG-82, supported by the Director for Energy Research, Office of Basic Energy Science.

REFERENCES

1. Synthesis, structure, and properties of $\text{Sr}_2\text{CuO}_2\text{Cl}_2$
L.L. MILLER, X.L. WANG, S.X. WANG, C. STASSIS, and D.C. JOHNSTON, *Phys. Rev. B* 41, pp. 1921-1925 (1990).
2. Antiferromagnetism in $\text{Sr}_2\text{CuO}_2\text{Cl}_2$
D. VAKNIN, S.K. SINHA, C. STASSIS, L.L. MILLER, and D.C. JOHNSTON, *Phys. Rev. B* 41, pp. 1926-1933 (1990).
3. μ^+ SR studies on $\text{Sr}_2\text{CuO}_2\text{Cl}_2$, La_2CuO_4 , and Nd_2CuO_4 : 2-d magnetism, local fields and muon sites
L.P. LE, G.M. LUKE, B.J. STERNLIEB, Y.J. UEMURA, J.H. BREWER, T.M. RISEMAN, D.C. JOHNSTON, L.L. MILLER, Y. HIDAKA, and H. MURAKAMI, *Hyperfine Interactions* 63, pp. 279-285 (1990).
4. ^{35}Cl NMR study of spin dynamics in $\text{Sr}_2\text{CuO}_2\text{Cl}_2$
F. BORSA, M. CORTI, T. GOTO, A. RIGAMONTI, D.C. JOHNSTON, and F.C. CHOU, *Phys. Rev. B* 45, pp. 5756-5759 (1992).
5. Antiferromagnetic form factor of $\text{Sr}_2\text{CuO}_2\text{Cl}_2$
X.L. WANG, L.L. MILLER, J. YE, C. STASSIS, B.N. HARMON, D.C. JOHNSTON, A.J. SCHULTZ and C.-K. LOONG, *J. Appl. Phys.* 67, pp. 4524-4526 (1990).
6. ^{35}Cl NMR study of magnetic ordering in $\text{Sr}_2\text{CuO}_2\text{Cl}_2$ single crystal
M. CORTI, F. BORSA, L.L. MILLER, and A. RIGAMONTI, *J. Appl. Phys.* (submitted Aug. 1993).
7. Muon-spin-rotation studies on single crystal $\text{Sr}_2\text{CuO}_2\text{Cl}_2$
L.P. LE, G.M. LUKE, B.J. STERNLIEB, Y.J. UEMURA, J.H. BREWER, T.M. RISEMAN, D.C. JOHNSTON, and L.L. MILLER, *Phys. Rev. B* 42, pp. 2182-2189 (1990).
8. Optical phonons in copper oxides with a single CuO_2 plane
S. TAJIMA, S. UCHIDA, S. ISHIBASHI, T. IDO, H. TAKAGI, T. ARIMA and Y. TOKURA, *Physica C* 168, pp. 117-122 (1990).
9. Normal state magnetism of the high T_c cuprate superconductors
See for example; D.C. JOHNSTON, *J. Magn. and Mag. Mat.* 100, pp. 218-240 (1991).
10. Zur kenntnis von $\text{Sr}_2\text{CuO}_2\text{Cl}_2$
VON B. GRANDE and H.K. MULLER-BUSCHBAUM, *Z. Anorg. Alleg. Chem.* 417, pp. 68-74 (1975).